

pubs.acs.org/JACS Article

Triple-Dearomative Photocycloaddition: A Strategy to Construct Caged Molecular Frameworks

Kaijie Ji, Jayachandran Parthiban, Steffen Jockusch, Jayaraman Sivaguru,* and John A. Porco, Jr.*



Cite This: J. Am. Chem. Soc. 2024, 146, 13445–13454



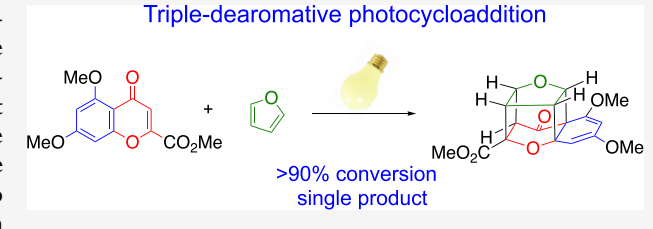
ACCESS

III Metrics & More

Article Recommendations

SI Supporting Information

ABSTRACT: An unprecedented caged 2*H*-benzo-dioxo-pentacy-cloundecane framework was serendipitously obtained in a single transformation via triple-dearomative photocycloaddition of chromone esters with furans. This caged structure was generated as part of an effort to access a tricyclic, oxygen-bridged intermediate enroute to the dihydroxanthone natural product nidulalin A. Reaction scope and limitations were thoroughly investigated, revealing the ability to access a multitude of synthetically challenging caged scaffolds in a



two-step sequence. Photophysical studies provided key mechanistic insights on the process for formation of the novel caged scaffold.

INTRODUCTION

Nidulalin A 1¹ and nidulaxanthone A 2² (Figure 1) belong to the dihydroxanthone natural product family. We have recently

Figure 1. Dihydroxanthone natural products.

reported total syntheses of 1 and 2 involving use of allyl triflate for chromone ester activation followed by vinylogous addition to access the nidulalin A scaffold in a four-step sequence, which also employs ketone desaturation using Bobbitt's oxoammonium salt.³ An initial approach to target monomer 1 involved use of chromone ester 3 as a substrate for Diels-Alder cycloaddition with furan to produce the intended cycloadduct 4 (Figure 2) followed by base-mediated carbon-oxygen bond cleavage to dienone 5 and subsequent demethylation. Herein, we report studies on the photochemical reactivity of chromone ester substrates such as 3 with furans, which led to the serendipitous discovery of a novel, triple-dearomative photocycloaddition to produce an underdeveloped, caged scaffold architecture.

RESULTS AND DISCUSSION

After unsuccessful trials with thermal cycloaddition of chromone ester 3 with furan, we envisioned that photomediated triplet Diels—Alder reaction^{4,5} of chromone ester 3⁶ may be employed to initiate the planned synthetic sequence illustrated in Figure 2. Interestingly, employing a 370 nm LED

light source and 4:1 MeCN/furan as a mixed solvent system (0.025 M), we unexpectedly obtained the novel caged compound 6 as the exclusive product with no evidence of Diels—Alder cycloadducts or *syn-, anti-*[2 + 2]-cycloaddition products (Table 1, entry 1). Compound 6 contains the dioxopentacycloundecane caged scaffold, which, to the best of our knowledge, has a single precedent in the literature⁷ from the work of West and co-workers as a minor product (7, 5% yield) (Figure 3A). The reaction pathway from 3 and furan to 6, an intermolecular triple-dearomative cycloaddition, ⁸ is unprecedented in the literature.

Polycyclic caged compounds have been widely used in medicinal chemistry, 9-17 and their intriguing structures often present challenges from a synthetic chemistry standpoint 10,13,14,16,18,19 (Figure 3B). For example, cubane 8 is a monoamine oxidase B (MAO-B) inhibitor and requires a 15-step synthesis; NGP1-01 9¹⁴ is a pentacycloundecane derivative with broad bioactivity 9-13,15,16,18 and requires a five-step synthesis; tromantadine 10²¹ is an adamantane derivative with antiviral activity and is synthesized in five steps. In comparison, caged compound 6 bearing the 2*H*-benzo-dioxo-pentacycloundecane (BDPC) moiety is synthesized in a one-step process from a chromone ester substrate and was found to be the only product in the reaction (Figure 3A).

In terms of reaction development, use of a 254 nm mercury lamp largely resulted in furan polymerization along with the

Received: February 22, 2024 Revised: April 19, 2024 Accepted: April 23, 2024 Published: May 6, 2024





Figure 2. Original synthetic plan for the synthesis of nidulalin A via cycloaddition of a chromone ester and furan.

Table 1. Discovery of Caged Compound 6 and Reaction Optimization Using Batch Conditions

entry	light source ^b	Solvent ^c	ratio	conc. (M)	irradiation time (h)	conv. (%) ^d	ratio of 6:11:12:3
1	370 nm	MeCN	4:1	0.025	20	100	100:0:0:0
2	254 nm	MeCN	4:1	0.025	2	48	44:3:0:57 ^e
3	370 nm	MeCN	4:1	0.050	20	100	97:3:0:0
4	370 nm	MeCN	4:1	0.100	20	100	80:20:0:0
5	370 nm	toluene	4:1	0.025	24	62	35:17:0:48
6	370 nm	TFE	4:1	0.025	24	0	0:0:0:100
7	390 nm	MeCN	4:1	0.025	20	65	65:0:0:35
8^f	427 nm	MeCN	4:1	0.025	24	27	0:0:27:73

"Reaction conducted on a 0.05 mmol scale. ^bA mercury lamp (150W) was employed in entry 2; Kessil lamps (40W) were employed in entries 1 and 3–8. ^cSolvents (MeCN, toluene or TFE) and furan were degassed for 20 min before use. ^dConversion and product ratio based on crude ¹H NMR analysis in neutralized CDCl₃. In all cases, only 6, 11, 12, and 3 were observed. Neutralized CDCl₃ was prepared via passing through a short basic alumina column. ^eFuran polymerization was observed as the major byproduct. ^fS mol % of thioxanthone included as additive.

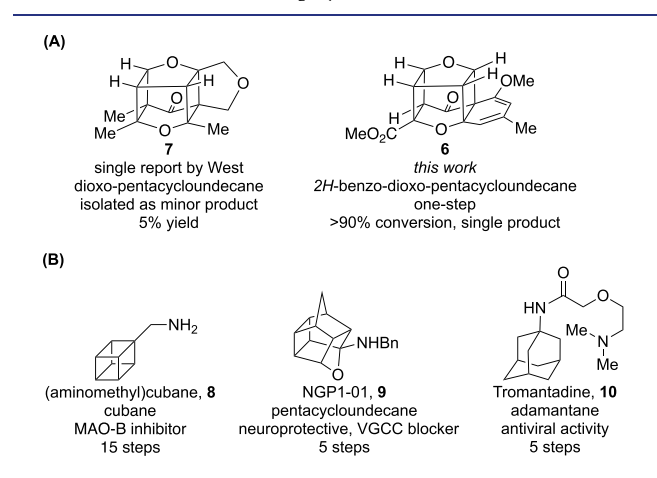


Figure 3. (A) Structural comparison of a precedented caged compound vs BDPC 6. (B) Select bioactive caged scaffolds in medicinal chemistry.

desired transformation (Table 1, entry 2). Conducting reactions at a higher concentration in MeCN (Table 1, entries 3 and 4), or in the nonpolar solvent toluene (Table 1, entry 5) resulted in the production of the chromone homodimer 11 as a minor product.²² Use of the protic solvent trifluoroethanol (TFE) totally mitigated reactivity and led to recovered chromone ester 3 (Table 1, entry 6). 23,24 Switching the light source from a 370 to 390 nm LED light source resulted in slower reactions (Table 1, entry 7). Employing the triplet photosensitizer thioxanthone (TX) using 427 nm photoirradiation instead resulted in the production of the chromonefuran [2 + 2]-syn adduct 12 (Table 1, entry 8). In order to increase light penetration and further improve conversion on a larger scale, we employed a flow photoreactor setup I, 25 which vastly improved the reaction efficiency and delivered the caged product 6 in 95% conversion within 3 h on a 75 mg reactionscale (Table 2, entry 2), which compares to a 67% conversion

Table 2. Reaction Optimization in Flow to Access Caged Compound 6

entry	reaction setup	ratio of MeCN:furan ^a	residence time (h)	conv. (%) ^b
1 ^c	batch	4:1	70	67
2^d	setup I	4:1	3	95
3^d	setup I	7:1	3	70
4 ^e	setup II	12:1	2	81
5 ^e	setup II	7:1	1	62
6 ^e	setup II	7:1	2.5	92

"MeCN and furan were degassed for 20 min before use. ^bConversion based on crude ¹H NMR analysis in neutralized CDCl₃. In all cases, only 3 and 6 were observed. CDCl₃ was neutralized by passing directly through a short basic Al₂O₃ column. ^c50 mg scale, batch setup using a 370 nm Kessil lamp. ^d75 mg scale, flow photoreactor setup I. ²⁵ ^e100 mg scale, flow photoreactor setup II (Figure 4²⁶). ²⁵

using batch conditions over 70 h on a 50 mg reaction scale (Table 2, entry 1). Further optimization using a 365 nm LED light source with a lower loading of furan (7:1 MeCN/furan) using the flow photoreactor setup II (Figure 4) developed by Beeler and co-workers^{25,26} led to a 92% conversion of 3 to 6 in 2.5 h residence time on a 100 mg reaction-scale (Table 2, entry 6).

Due to the instability of caged compound 6 in acidic environments which ultimately led to retro-[2+2]-[2+2] to chromone ester 3, we further functionalized scaffold 6 in order to stabilize the structure (Figure 5). We found that exposure of 6 to silica gel afforded the retro-[2+2] cycloadduct 12 along with chromone ester 3 as an inseparable mixture, thereby reinforcing the lability of the caged scaffold with its adjacent

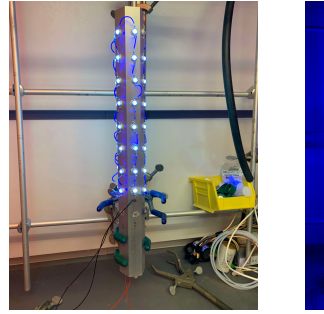




Figure 4. Pictures of flow photoreactor setup II.²⁶

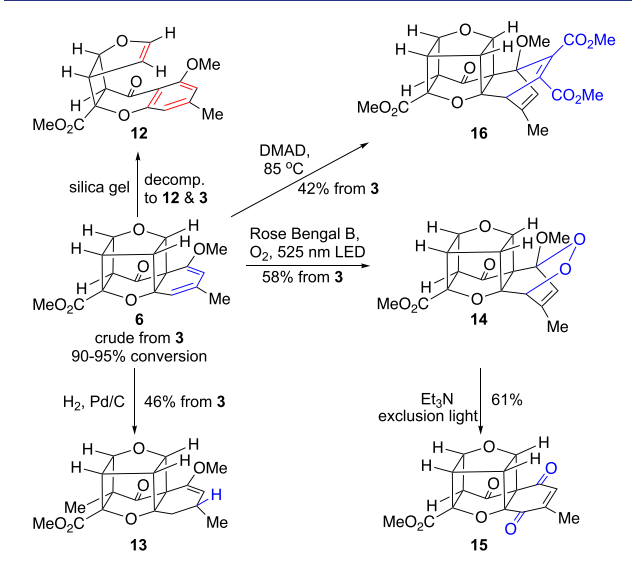


Figure 5. Production of a novel caged compound and further functionalization chemistry.

dienol ether moiety. Hydrogenation of 6 (Pd/C, H₂) afforded methyl enol ether 13 in 46% yield from 3 as a stable compound. Treatment of 6 under singlet oxygen conditions (Rose Bengal B, O₂, green LED) led to the endoperoxide 14 which was isolated as a stable, tan solid in 58% yield from 3. The intriguing hydrogenated 2,7-dioxa-1,2b-methanobenzo-[1,4]cyclobuta[1,2,3-cd]cyclobuta[gh]pentalene framework of 14 was unambiguously confirmed by single X-ray crystallographic analysis (Figure 6). Kornblum—DeLaMare rearrangement²⁷ of 14 employing triethylamine (Et₃N) as base with exclusion of light led to clean conversion of 14 to enedione 15 in 61% yield. Finally, Diels—Alder cycloaddition of 6 with dimethyl acetylenedicarboxylate (DMAD) afforded diester 16 in 42% yield (Figure 5). It should be noted that DMAD and singlet oxygen were sufficiently small in size to react with the

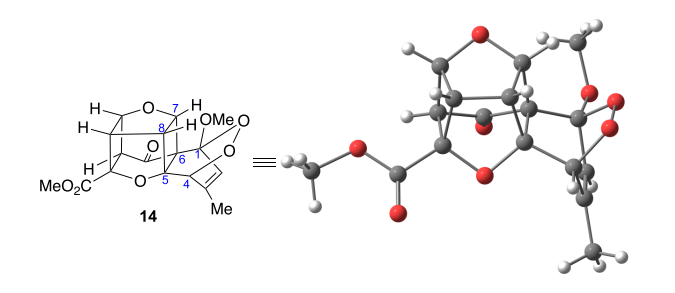


Figure 6. X-ray crystal structure of 14.

congested dienol ether moiety of **6** in comparison to other dienophiles evaluated (e.g., maleic anhydride and benzoquinone). Moreover, Diels—Alder cycloaddition exclusively took place from the top face of caged compound **6** adjacent to the "ledge" provided by the diene and the adjacent cyclobutane ring. Based on examination of substrate and product structures, the excellent stereoselectivity for reactions affording products such as **14** and **16** may be due to the electrostatic repulsion of the oxygens (*shown in red*) in substrate **6** (Figure 7) with oxygenated reaction partners such as singlet oxygen and DMAD. ^{28,29}

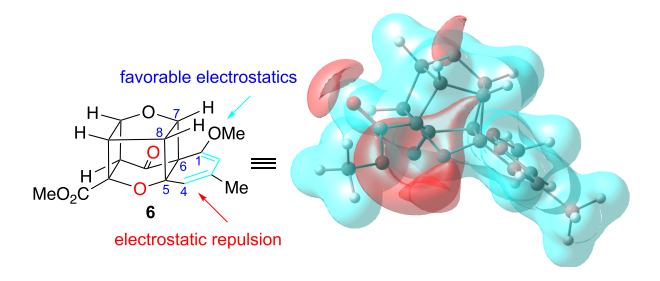


Figure 7. Map of the electrostatic potential (MEP) of BDPC 6.

With optimized conditions in hand, we next explored the substrate scope of heterocyclic reaction partners by using optimized batch or flow conditions (Table 3, vide infra). Furan substrates including 2-substituted and 2,5-disubstituted furans 17 - 20 participated as reaction partners to afford the corresponding caged compounds (not shown), with lower conversions observed upon increasing steric hindrance (entries 1-4). The caged compounds obtained were further functionalized to the stable derivatives 21 - 23 and 25 - 26 using previous developed conditions (cf. Figure 5). Use of 2methylfuran 17 as a reaction partner afforded a 1:1 mixture of isomeric enol ethers 21 and 22 (34% yield, inseparable) after hydrogenation (Table 3, entry 1). The corresponding caged compound from 3 and 2,5-dimethylfuran 18 afforded methyl enol ether 23 in 27% yield after hydrogenation (Table 3, entry 2). The caged compound 24 derived from 2-trimethylsilyl furan 19 was found to be very labile under mild acidic conditions and readily afforded the retro-[2 + 2] cycloadduct 25 in 49% yield by treatment in CDCl₃ (50 °C) (Table 3, entry 3). 2-Trimethylsilyl-5-methylfuran 20 afforded the corresponding caged compound as single regioisomer, likely due to the steric hindrance and blocking effect of the trimethylsilyl (TMS) group.³⁰ Similar to the production of 25 from 24, cyclobutane-opening product 26 was isolated in 35% yield after treatment with CDCl₃ (50 °C) (Table 3, entry 4).

Mechanistically, we believe that cyclobutane edge protonation 31,32 in the presence of adventitious D-Cl may open the cyclobutane ring of **24** to a transient cation **27**, which is stabilized by the silicon β -effect 33,34 followed by elimination and aromatization to afford product **25** (Figure 8B). Originally, we considered that **25** may be converted back to **24** *via* dearomative [2 + 2]-cycloaddition as DFT computational analysis (r²SCAN-3C/CPCM (CH₂Cl₂)) of **25** showed a close distance between the corresponded alkene and the two carbons of the arene (Figure 8C). However, all attempts including photoirradiation **25** using a 365 nm LED or a white LED in MeCN or thermolysis failed to deliver **24** but instead led to

Table 3. Heterocycle Substrate Scope

Entry	Heterocycle	Batch/flow a	Reaction time (h)	Conv.(%) ^b	Condition c	Product	Yield (%) ^d
1	0 Me 17	batch	42	100	A	H O Me Me O H OME ME O ME O ME ME O	34
2	Me Me	batch	46	95	A	Me O H OMe H OMe H OMe H MeO ₂ C NMe	27
3	0 TMS	flow	6	67	В	H O TMS OMe OMe MeO ₂ C O Me	49
4	Me O TMS	batch	44	90	В	MeO ₂ C Me	35
5	CO ₂ Me	batch	78	53	С	CO ₂ Me H HOMe O HOMeO ₂ C 29 Me	27

"Flow conditions employing 0.4 mmol of 3; batch conditions employing 0.1 mmol of 3. "Conversion measured by the crude ¹H NMR from the initial photochemical reaction with chromone ester 3. "Condition A: 2 mol % Pd/C, H₂, EtOAc. Condition B: CDCl₃, 50 °C, 36 h. Condition C: 5 mol % Rose Bengal B, O₂, CDCl₃/CD₃OD = 9:1, 525 nm LED. "Yield over two steps from chromone ester 3."

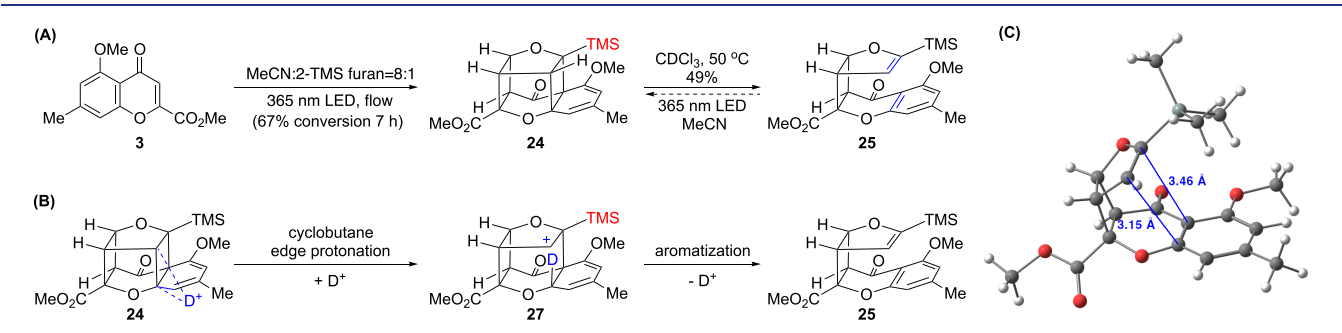


Figure 8. (A) Irreversible retro-[2 + 2]-cycloadduct 25 formation facilitated by cyclobutane edge protonation. (B) Proposed mechanism for formation of 25. (C) DFT structure of compound 25 ($r^2SCAN-3C/CPCM$ (CH_2Cl_2)).

recovery of starting material which indicated an irreversible process for formation of 25 (Figure 8A).

Regarding additional substrate scope, use of 3-substituted, 2,3-disubstituted or 3,4-disubstituted furans (cf. Table S5) $^{2.5}$ failed to deliver the desired corresponding caged compounds in all cases, likely due to increasing steric hindrance of the 3-furyl substituents. We also found that N-(methoxycarbonyl)-pyrrole 28 could serve as reaction partner with 3 to afford the corresponding caged nitrogen-containing scaffold in lower conversion with elongated reaction time (53% conversion, 78 h in batch). Fortunately, the corresponding endoperoxide 29 from this caged intermediate could be isolated in 27% yield (vide supra, Table 3, entry 5). Unfortunately, thiophene

substrates and electron-rich, *N*-substituted pyrroles such as *N*-methyl and *N*-trimethylsilyl pyrrole failed to deliver related caged compounds under similar conditions (*cf.* Table S5).²⁵

We next explored substrate scope using various chromone substrates 30 – 34 (Table 4), which involved processing of the corresponding crude, caged products using conditions developed in Figure 5. Switching the methyl group of chromone 3 into a hydrogen (30) or a methoxy group (31) did not interfere with the formation of the caged products. Accordingly, endoperoxide 35 was generated in 45% yield from 30 using flow conditions followed by endoperoxidation (Table 4, entry 1). We also found that diene 36 from dimethoxy chromone ester substrate 31 was a relatively stable caged

Table 4. Chromone Substrate Scope^a

Entry	Chromone substrate	Batch/ flow	Reaction time (h)	Conv. (%) b	Condition ^c	Product	Yield (%) d
1	OMe O CO ₂ Me	flow	2.5	91	A	H HOMEO HOMEO MeO ₂ C 35	45
2			67	88	В	HO ₂ C OMe 36 (35%) + 37 (10%)	45
3	OMe O OCO ₂ Me	batch	07	00	С	H O H OME CO ₂ Me H OME CO ₂ Me CO ₂ Me OME OME	54
4			45	80	A	H O H OMe H OMe MeO ₂ C 37	23
5	Me OCO ₂ Me	batch	24	67	A	HOBN O HOBN O MeO ₂ C 39 Me	36
6	MOMO O Me O CO ₂ Me	batch	44	75	A	H O H OMOM O O O O O O O O O O O O O O O	47
7	OMe O NHnBu 34	batch	47	67	D	Buhn H O H OME O 41	50

[&]quot;Flow conditions employing 0.4 mmol of chromone substrate; batch conditions employing 0.1 mmol of chromone substrate. "Conversion measured by crude ¹H NMR analysis from the initial photochemical reaction with furan. "Condition A: 5 mol % Rose Bengal B, O₂, CDCl₃/CD₃OD = 9:1, 525 nm LED. Condition B: silica gel. Condition C: 10 equiv. DMAD, toluene, 85 °C. Condition D: 2 mol % Pd/C, H₂, EtOAc. "Yield over two steps from chromone ester."

product on silica gel and could be isolated in 35% yield together with 10% of the hydrolyzed methoxy enone 37 produced by acid hydrolysis on silica gel (Table 4, entry 2). Thermolysis of 36 with DMAD afforded cycloadduct 38 in 54% yield (Table 4, entry 3). Interestingly, the hydrolysis product 3-methoxy cyclohex-2-enone 37 was isolated as the exclusive product in 23% yield from crude 36 using Rose Bengal B/O2 conditions; we did not observe the expected endoperoxide as in other cases (Table 4, entry 4). Rose Bengal-catalyzed demethylation and photocatalytic hydrolysis of enol ethers have been reported in the literature. 35,36 Switching the peri-methoxy group of 3 into a peri-benzyloxy (32) or a peri-methoxymethyl group (33) led to similar results in comparison to substrate 3 affording endoperoxides 39 and 40 in 36% and 47% yields, respectively, using batch conditions followed by endoperoxidation (Table 4, entries 5 and 6).

Switching the ester moiety of 3 into an amide (34) resulted in similar reactivity; the corresponding caged compound was further reduced to enol ether 41 in 50% yield by using Pd/C/ H_2 (Table 4, entry 7). Unfortunately, switching the R_1 substituent of 3 from methoxy to other functional groups (e.g. H, OH, or OAc) or changing the R_2 group of 3 from an ester into other functional groups (e.g. H, Ph or CN) failed to deliver the corresponding caged products (cf. Table S6).²⁵

To gain additional insight into the formation of caged compound 6 and its derivatives, we performed a detailed photophysical investigation using the key reaction partner 3. Chromone ester 3 absorbs light below ~ 390 nm and shows two peaks at 325 and 274 nm with molar absorptivities of 6728 and 18117 M⁻¹cm⁻¹, respectively (Figure 9A, blue line). Addition of furan to solutions of 3 did not cause significant changes in absorbance above 300 nm, indicating that no

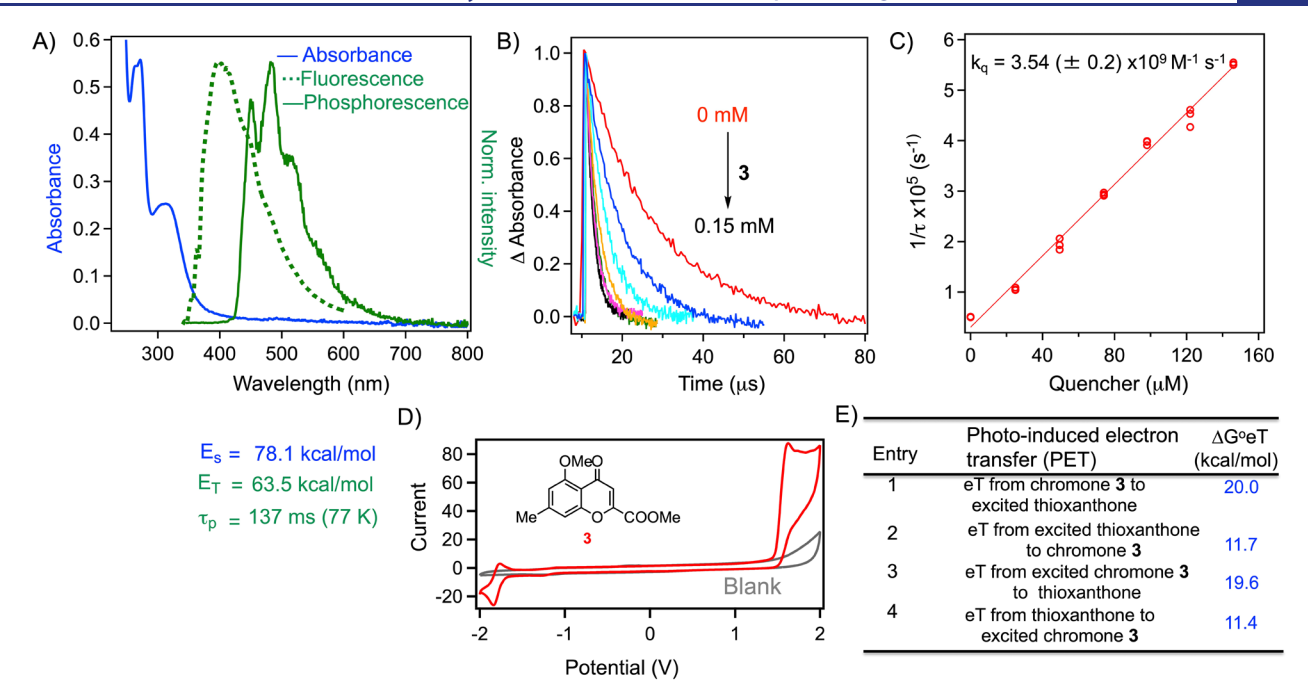


Figure 9. (A) UV—vis absorption spectrum in EtOH at rt (blue); fluorescence spectrum in EtOH ($\lambda_{\rm ex}$ = 325 nm) at rt (dotted; green); time-resolved phosphorescence spectrum recorded 5–55 ms after pulsed excitation at 325 nm in EtOH glass at 77 K (solid; green). (B) Thioxanthone triplet decay traces (Δ absorbance) monitored at 620 nm measured by laser flash photolysis ($\lambda_{\rm ex}$ = 355 nm, 7 ns pulse width) in the absence and presence of different concentrations of 3 in argon saturated CH₃CN solutions. (C) Determination of the bimolecular quenching rate constant $k_{\rm q}$ of quenching of thioxanthone triplet states by 3 using the kinetic data shown in (B). Plot of the inverse triplet lifetime vs concentration of 3. (D) CV experiments for 3. (E) Free energy for electron transfer under sensitized conditions.

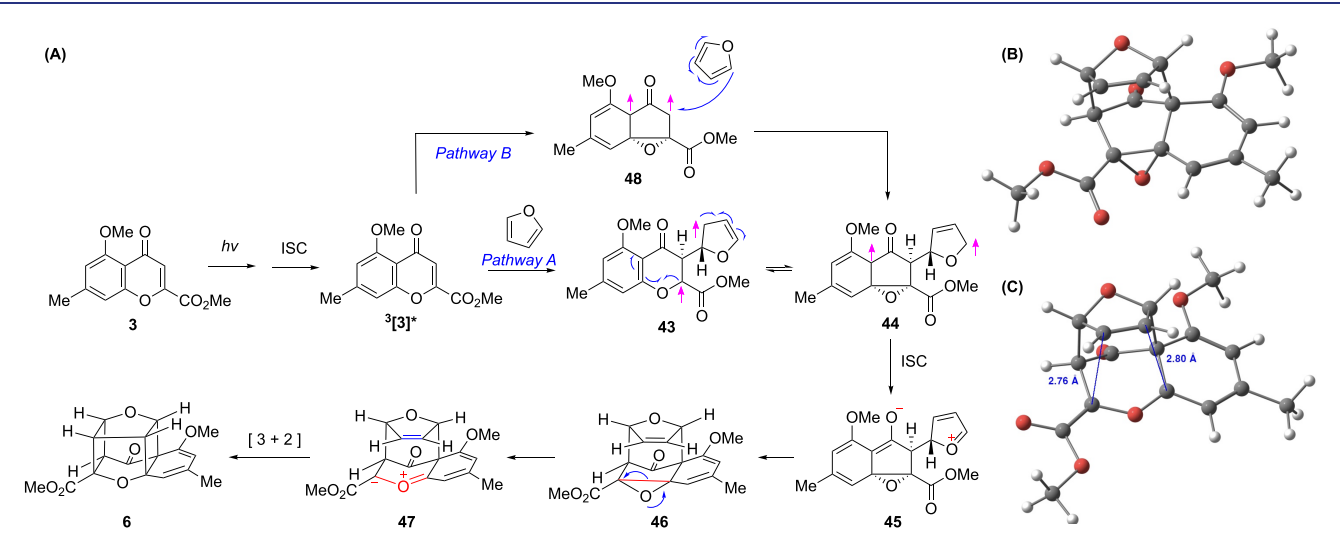


Figure 10. (A) Proposed mechanism for the formation of 6. (B) DFT computations of oxirane 46 (r²SCAN-3C/CPCM (CH₂Cl₂)). (C) DFT computations of carbonyl ylide 47 (r²SCAN-3C/CPCM (CH₂Cl₂)).

ground state EDA complexes³⁷ are formed between 3 and furan.²⁵ Having ascertained that the reaction does not proceed via ground state EDA complex formation, the excited state properties of 3 were further investigated.²⁵ Photoexcitation of 3 at 330 nm generated weak fluorescence (Figure 9A, dotted green line). The energy of the lowest singlet excited state of 3 (78.1 kcal/mol⁻¹) was estimated from the intercept of the absorption and fluorescence spectra (Figure S4).²⁵ The low fluorescence quantum yield (<0.005), determined by comparison to the standard (9,10-diphenylanthracene),³⁸ indicates fast singlet excited state deactivation processes including intersystem crossing (ISC) into the triplet state. Phosphor-

escence studies were performed to investigate the formation and energy of the triplet states. Figure 9A (green line) shows the phosphorescence spectrum of 3 at 77 K in an EtOH matrix, and it has a lifetime of 137 ms. The energy of the triplet state was determined from the highest-energy peak (63.5 kcal/mol). These point to the $\pi\pi^*$ nature of the lowest triplet excited state. It is possible that the $n\pi^*$ triplet state is close in energy to the $\pi\pi^*$ triplet state resulting in intermixing. Such a scenario for 3 is similar to the excited state features of enone derivatives. This may be a key reason the fluorescence quantum yield was low in 3 coupled with a strong phosphorescence. As shown above, the photoreaction

proceeded efficiently in the presence of TX 42 as triplet sensitizer. 40 We then determined the bimolecular quenching rate constant of the TX triplet states by 3 using laser flash photolysis. Laser excitation ($\bar{\lambda}_{ex} = 355$ nm, pulse width = 7 ns) of an argon-saturated solution of TX in acetonitrile generated a triplet transient absorption centered at ~620 nm, 41 which was quenched by 3 (Figure 9B). The bimolecular quenching rate constant was determined from the slope of the plot of the inverse triplet lifetimes vs the concentration of 3 which gave a close to diffusion-controlled rate constant ($k_q = 3.54 (\pm 0.2) \times$ 10⁹ M⁻¹ s⁻¹; Figure 9C). The quenching of triplet excited states by 3 may proceed by energy or electron transfer. As the triplet energy of the sensitizer thioxanthone 42 (TX = 64 kcal/ (3 = 63.5 kcal/mol) are close, ²⁵ one can anticipate energy transfer from the sensitizer to the chromone ester substrate. By using the Rehm-Weller equation, we also evaluated the viability of photoinduced electron transfer (PET) playing a role under sensitized conditions. Inspection of the Table (Figure 9E) revealed an endergonic electron transfer from excited sensitizer 42 (³TX*) to chromone 3 as well as triplet excited chromone $(^{3}3^{*})$ to sensitizer 42 (TX). Due to the highly endergonic nature of electron transfer in the reaction of TX triplets with 3 and the close to diffusion-controlled rate constant of ³TX* quenching by 3, energy transfer is the most likely pathway for the reaction generating triplet-excited states of 3. In addition, the photoexcited reduction potential of 3 was calculated to be +0.91 V by use of the Rehm-Weller approximation, which is insufficient to oxidize furan ($E_{\rm ox} = +1.80~{\rm V}$). As was previously mentioned, *N*-methyl pyrrole ($E_{\rm ox} = +1.09~{\rm V}$) with a closer oxidative potential to the photoexcited state of 3 failed to deliver the corresponding caged compound with 3 but rather returned the starting material. As a result, only the triplet excited state of substrate 3 appears to be involved in the formation of caged scaffold 6.

As we established the formation of the triplet excited state of 3 upon direct irradiation through photophysical studies, we propose a mechanism for the formation of the caged photoproduct 6 (Figure 10). As a working hypothesis, we believe that triplet excited chromone ³[3]* is generated upon direct irradiation of 3. This is reasonable, as we observed a very weak fluorescence of 3 with low quantum yields. The tripletexcited chromone 3[3]* subsequently reacts with furan to generate triplet biradial species 43 (Figure 10). This triplet diradical 43 undergoes dearomative cyclization leading to 44 followed by intersystem crossing (ISC) to form the zwitterionic intermediate 45. This intermediate 45 undergoes cyclization to 46 (Figure 10), which may subsequently ringopen to carbonyl ylide 42,43 47 (Figure 10) which may be followed by intramolecular (3 + 2) cycloaddition^{42,43} to the caged cycloadduct 6 (Figure 10, Pathway A). An alternative mechanism (Figure 10, Pathway B) can be envisioned for the formation of 6 that features the tautomeric, dearomatized triplet diradical intermediate 48 generated from the triplet excited chromone ³[3]*, which is reminiscent of diradical intermediates observed and proposed in oxa-di- π -methane rearrangements of substrates including cyclohexadienones.⁴⁴ The diradical intermediate 48 may react with furan in a stepwise fashion (as it occurs in a triplet manifold) to form triplet biradical 44. This triplet biradical 44 intersystem crosses to zwitterionic species 45 enroute to the formation of cycloadduct 6. A point to note is that diradical intermediate 48 can also intersystem cross to an oxyallyl cation type species

(similar to the intermediates proposed by West and coworkers)⁷ followed by formal addition of furan to form intermediate **46**.

To validate and further study the proposed mechanism depicted in Figure 10, we carried out the series of control studies detailed in Figure 11A,B). In the first experiment

Figure 11. (A) Mechanistic studies involving thioxanthone 42. (B) Radical clock experiment to probe HAT.

(Figure 11A), we employed triplet energy transfer by utilizing thioxanthone 42 ($E_T = 64 \text{ kcal/mol}$) as the triplet photosensitizer to generate triplet excited chromone ${}^{3}[3]^{*}$ that was established to have a triplet energy of ~63.5 kcal/mol (Figure 11A). Sensitized irradiation of chromone 3 under energy transfer conditions with thioxanthone 42 in the presence of furan in acetonitrile (MeCN/furan = 4:1) resulted in the formation of [2 + 2]-photoproduct 12. To rationalize the formation of [2 + 2]-photoproduct 12 under triplet sensitization, we subjected the caged photoadduct 6 to sensitized irradiation with thioxanthone 42 and were able to observe the formation of [2 + 2]-photoproduct 12. This is due to the fact that **6** features a diene chromophore ⁴⁵ that likely has a triplet $\pi\pi^*$ excited state with energy similar to that of thioxanthone 42. Specifically, triplet-excited 6 generated upon energy transfer from thioxanthone⁴⁶ undergoes β -cleavage resulting in the formation of the [2 + 2]-photoproduct 12. Alternatively, an electron transfer from the diene 6 to the excited thioxanthone followed by cleavage of the dienyl-cation, resulting in the formation of the [2 + 2]-photoproduct 12 cannot be ruled out. In the second of experiments (Figure 11B), the cyclopropyl chromone radical clock substrate 49 was subjected to direct irradiation, which resulted in the formation of aldehyde 50, albeit in 11% yield. The formation of 49 can be rationalized by intramolecular H atom abstraction from the triplet excited chromone ³[49]* to generate diradical 51,

which may be followed by spirocyclization to intermediate 52 and elimination/rearomatization. The latter experiment once again reinforces that the triplet excited state of 3 and related chromone esters have $\pi\pi^*$ character intermixed with the higher lying $n\pi^*$ triplet excited state as observed in our photophysical studies.

CONCLUSIONS

In summary, we serendipitously discovered and synthesized an unprecedented caged architecture bearing the 2H-benzodioxo-pentacycloundecane (BDPC) scaffold in a single transformation from photoirradiation of chromone esters and furans via a triple-dearomative cycloaddition process. Flow photoreactors were employed for reaction scale-up, and a series of subsequent functionalizations of the caged scaffold were developed in a one-pot, two-step manner. Overall, 25 caged compounds were prepared in yields ranging from 27-58%, encompassing variations of both chromone and heterocycle substrates. Photophysical studies provided key mechanistic insights into the process for formation of this caged scaffold. We believe that the novel compounds produced in this study should provide further impetus for research on the rapid synthesis of caged structures for use in drug discovery and medicinal chemistry. Further studies on the chemistry of the caged BDPC architecture as well as biological evaluation of the scaffolds are currently in progress and will be reported in due

ASSOCIATED CONTENT

Supporting Information

The Supporting Information is available free of charge at https://pubs.acs.org/doi/10.1021/jacs.4c02674.

> Experimental procedures, analytical data, and ¹H and ¹³C NMR spectra of all newly synthesized compounds, X-ray crystallographic data for endoperoxide 14 and DMAD adduct 38, DFT calculation details, and photophysical studies (PDF)

Accession Codes

CCDC 2333098-2333099 contain the supplementary crystallographic data for this paper. These data can be obtained free of charge via www.ccdc.cam.ac.uk/data request/cif, or by emailing data_request@ccdc.cam.ac.uk, or by contacting The Cambridge Crystallographic Data Centre, 12 Union Road, Cambridge CB2 1EZ, UK; fax: +44 1223 336033.

AUTHOR INFORMATION

Corresponding Authors

Jayaraman Sivaguru - Department of Chemistry and Center for Photochemical Sciences, Bowling Green State University, Bowling Green, Ohio 43403, United States; Email: sivagj@ bgsu.edu

John A. Porco, Jr. - Department of Chemistry and Center for Molecular Discovery (BU-CMD), Boston University, Boston, Massachusetts 02215, United States; Email: porco@bu.edu

Authors

Kaijie Ji – Department of Chemistry and Center for Molecular Discovery (BU-CMD), Boston University, Boston, Massachusetts 02215, United States

Jayachandran Parthiban - Department of Chemistry and Center for Photochemical Sciences, Bowling Green State University, Bowling Green, Ohio 43403, United States

Steffen Jockusch – Department of Chemistry and Center for Photochemical Sciences, Bowling Green State University, Bowling Green, Ohio 43403, United States; o orcid.org/ 0000-0002-4592-5280

Complete contact information is available at: https://pubs.acs.org/10.1021/jacs.4c02674

Funding

R35 GM 118173 (NIH) CHE-1955524 (NSF)

The authors declare no competing financial interest.

ACKNOWLEDGMENTS

K.J. and J.A.P, Jr. thank the National Institutes of Health (NIH) (R35 GM 118173) for financial support. We thank Dr. Jeffrey Bacon (Boston University) for assistance with X-ray crystal structure analysis and Professor Aaron Beeler and Dr. Matthew Mailloux (Boston University) for help with flow photoreactor construction and use. We thank the National Science Foundation (NSF) for support and Professor Joseph Derosa and Dr. James McNeely (Boston University) for helpful discussions. We thank the NMR (CHE-0619339) and MS (CHE-0443618) facilities at BU and the NIH (S10OD028585) for support of a single-crystal XRD system. Computational work at Boston University reported in this paper was performed on the Shared Computing Cluster (SCC), which is administered by Boston University's Research Computing Services. J.S. thanks the National Science Foundation for generous support for his research program (CHE-1955524) and for the purchase of excitation sources used in the photophysical experiments. J.P. thanks the Center for Photochemical Sciences for a Taller Fellowship.

REFERENCES

- (1) Kawahara, N.; Sekita, S.; Satake, M.; Udagawa, S. I.; Kawai, K. I. Structures of a New Dihydroxanthone Derivative, Nidulalin A, and a New Benzophenone Derivative, Nidulalin B, from Emericella Nidulans. Chem. Pharm. Bull. 1994, 42 (9), 1720-1723.
- (2) Wang, F.; Jiang, J.; Hu, S.; Hao, X.; Cai, Y.; Ye, Y.; Ma, H.; Sun, W.; Cheng, L.; Huang, C.; Zhu, H.; Zhang, H.; Zhang, G.; Zhang, Y. Nidulaxanthone A, a Xanthone Dimer with a Heptacyclic 6/6/6/6/ 6/6 Ring System from Aspergillus Sp.-F029. Org. Chem. Front. 2020, 7 (7), 953-959.
- (3) Ji, K.; Johnson, R. P.; McNeely, J.; Al Faruk, M.; Porco, J. A. Asymmetric Synthesis of Nidulalin A and Nidulaxanthone A: Selective Carbonyl Desaturation Using an Oxoammonium Salt. J. Am. Chem. Soc. 2024, 146 (7), 4892-4902.
- (4) Shaik, S. S.; Epiotis, N. D. Spin Inversion in Triplet Diels-Alder Reactions. J. Am. Chem. Soc. 1980, 102 (1), 122-131.
- (5) González-Béjar, M.; Stiriba, S.-E.; Domingo, L. R.; Pérez-Prieto, J.; Miranda, M. A. Mechanism of Triplet Photosensitized Diels-Alder Reaction between Indoles and Cyclohexadienes: Theoretical Support for an Adiabatic Pathway. J. Org. Chem. 2006, 71 (18), 6932-6941.
- (6) Sakamoto, M.; Yagishita, F.; Kanehiro, M.; Kasashima, Y.; Mino, T.; Fujita, T. Exclusive Photodimerization Reactions of Chromone-2-Carboxylic Esters Depending on Reaction Media. Org. Lett. 2010, 12 (20), 4435-4437.
- (7) West, F. G.; Hartke-Karger, C.; Koch, D. J.; Kuehn, C. E.; Arif, A. M. Intramolecular [4 + 3]-Cycloadditions of Photochemically Generated Oxyallyl Zwitterions: A Route to Functionalized Cyclooctanoid Skeletons. J. Org. Chem. 1993, 58 (24), 6795-6803.
- (8) For Examples of Double Dearomative Cycloadditions, See: (a) Zhu, M.; Xu, H.; Zhang, X.; Zheng, C.; You, S.-L. Visible-Light-Induced Intramolecular Double Dearomative Cycloaddition of Arenes. Angew. Chem., Int. Ed. 2021, 60 (13), 7036-7040.

- (b) Zhen, G.; Zeng, G.; Jiang, K.; Wang, F.; Cao, X.; Yin, B. Visible-Light-Induced Diradical-Mediated Ipso-Cyclization towards Double Dearomative [2 + 2]-Cycloaddition or Smiles-Type Rearrangement. Chem. - Eur. J. 2023, 29 (15), No. e202203217.
- (9) Van der Schyf, C. J.; Geldenhuys, W. J. Polycyclic Compounds: Ideal Drug Scaffolds for the Design of Multiple Mechanism Drugs? Neurotherapeutics. 2009, 6 (1), 175-186.
- (10) Young, L.-M.; Geldenhuys, W. J.; Domingo, O. C.; Malan, S. F.; Van der Schyf, C. J. Synthesis and Biological Evaluation of Pentacycloundecylamines and Triquinylamines as Voltage-Gated Calcium Channel Blockers. Arch. Pharm. (Weinheim). 2016, 349 (4), 252–267.
- (11) Beinat, C.; Banister, S. D.; Hoban, J.; Tsanaktsidis, J.; Metaxas, A.; Windhorst, A. D.; Kassiou, M. Structure-Activity Relationships of N-Substituted 4-(Trifluoromethoxy)Benzamidines with Affinity for GluN2B-Containing NMDA Receptors. Bioorg. Med. Chem. Lett. 2014, 24 (3), 828-830.
- (12) Zindo, F. T.; Barber, Q. R.; Joubert, J.; Bergh, J. J.; Petzer, J. P.; Malan, S. F. Polycyclic Propargylamine and Acetylene Derivatives as Multifunctional Neuroprotective Agents. Eur. J. Med. Chem. 2014, 80, 122 - 134.
- (13) Zindo, F. T.; Malan, S. F.; Omoruyi, S. I.; Enogieru, A. B.; Ekpo, O. E.; Joubert, J. Design, Synthesis and Evaluation of Pentacycloundecane and Hexacycloundecane Propargylamine Derivatives as Multifunctional Neuroprotective Agents. Eur. J. Med. Chem. 2019, 163, 83-94.
- (14) Geldenhuys, W. J.; Malan, S. F.; Murugesan, T.; Van der Schyf, C. J.; Bloomquist, J. R. Synthesis and Biological Evaluation of Pentacyclo [5.4.0.02,6.03,10.05,9] Undecane Derivatives as Potential Therapeutic Agents in Parkinson's Disease. Bioorg. Med. Chem. 2004, 12 (7), 1799-1806.
- (15) Joubert, J.; Geldenhuys, W. J.; Van der Schyf, C. J.; Oliver, D. W.; Kruger, H. G.; Govender, T.; Malan, S. F. Polycyclic Cage Structures as Lipophilic Scaffolds for Neuroactive Drugs. Chem-MedChem. 2012, 7 (3), 375-384.
- (16) Kapp, E.; Joubert, J.; Sampson, S. L.; Warner, D. F.; Seldon, R.; Jordaan, A.; de Vos, M.; Sharma, R.; Malan, S. F.; Khong, H. Y. Antimycobacterial Activity, Synergism, and Mechanism of Action Evaluation of Novel Polycyclic Amines against Mycobacterium Tuberculosis. Adv. Pharmacol. Pharm. Sci. 2021, 2021, 1.
- (17) Ragshaniya, A.; Kumar, V.; Tittal, R. K.; Lal, K. Nascent Pharmacological Advancement in Adamantane Derivatives. Arch. Pharm. 2023, No. e2300595.
- (18) James, B.; Viji, S.; Mathew, S.; Nair, M. S.; Lakshmanan, D.; Ajay Kumar, R. Synthesis of Novel Highly Functionalized Biologically Active Polycyclic Caged Amides. Tetrahedron Lett. 2007, 48 (35), 6204-6208.
- (19) Bliese, M.; Tsanaktsidis, J. Dimethyl Cubane-1,4-Dicarboxylate: A Practical Laboratory Scale Synthesis. Aust. J. Chem. 1997, 50 (3),
- (20) Silverman, R. B.; Zhou, J. P.; Eaton, P. E. Inactivation of Monoamine Oxidase by (Aminomethyl)Cubane. First Evidence for an.alpha.-Amino Radical during Enzyme Catalysis. J. Am. Chem. Soc. 1993, 115 (19), 8841-8842.
- (21) Rosenthal, K. S.; Sokol, M. S.; Ingram, R. L.; Subramanian, R.; Fort, R. C. Tromantadine: Inhibitor of Early and Late Events in Herpes Simplex Virus Replication. Antimicrob. Agents Chemother. **1982**, 22 (6), 1031–1036.
- (22) Sakamoto, M.; Kanehiro, M.; Mino, T.; Fujita, T. Photodimerization of Chromone. Chem. Commun. 2009, 17, 2379-2380.
- (23) (a) Wagner, P. J.; Truman, R. J.; Scaiano, J. C. Substituent Effects on Hydrogen Abstraction by Phenyl Ketone Triplets. J. Am. Chem. Soc. 1985, 107 (24), 7093-7097. (b) Wagner, P. J.; Puchalski, A. E. Quenching of Triplet Ketones by Alcohol Hydroxy Bonds. J. Am. Chem. Soc. 1980, 102 (23), 7138-7140.
- (24) Dauben, W. G.; Spitzer, W. A.; Kellogg, M. S. Photochemistry of 4-methyl-4-phenyl-2-cyclohexenone. Effect of solvent on the excited state. J. Am. Chem. Soc. 1971, 93 (15), 3674-3677.

- (25) Please see the Supporting Information for complete experimental details.
- (26) Lenihan, J. M.; Mailloux, M. J.; Beeler, A. B. Multigram Scale Synthesis of Piperarborenines C-E. Org. Process. Res. Dev. 2022, 26 (6), 1812–1819.
- (27) Kornblum, N.; DeLaMare, H. E. The Base Catalyzed Decomposition of A Dialkyl Peroxide. J. Am. Chem. Soc. 1951, 73 (2), 880-881.
- (28) Soleymani, M. A Density Functional Theory Study on the [3 + 2] Cycloaddition of N-(p-Methylphenacyl)Benzothiazolium Ylide and 1-Nitro-2-(p-Methoxyphenyl) Ethene: The Formation of Two Diastereomeric Adducts via Two Different Mechanisms. Theor. Chem. Acc. 2019, 138 (7), 87.
- (29) Suresh, C. H.; Remya, G. S.; Anjalikrishna, P. K. Molecular Electrostatic Potential Analysis: A Powerful Tool to Interpret and Predict Chemical Reactivity. WIREs Comput. Mol. Sci. 2022, 12 (5),
- (30) Schreiber, S. L.; Desmaele, D.; Porco, J. A. On the Use of Unsymmetrically Substituted Furans in the Furan-Carbonyl Photocycloaddition Reaction: Synthesis of a Kadsurenone-Ginkgolide Hybrid. Tetrahedron Lett. 1988, 29 (51), 6689-6692.
- (31) Lee, C. C.; Ko, E. C. F. A Search for Protonated Cyclobutane. Can. J. Chem. 1976, 54 (11), 1722-1725.
- (32) Pakkanen, T.; Whitten, J. L. Theoretical Studies of the Protonation of Cyclobutane. J. Am. Chem. Soc. 1975, 97 (22), 6337-
- (33) Roberts, D. D.; McLaughlin, M. G. Strategic Applications of the β-Silicon Effect. Adv. Synth. Catal. 2022, 364 (14), 2307–2332.
- (34) Lambert, J. B.; Zhao, Y.; Emblidge, R. W.; Salvador, L. A.; Liu, X.; So, J.-H.; Chelius, E. C. The β Effect of Silicon and Related Manifestations of σ Conjugation. Acc. Chem. Res. 1999, 32 (2), 183–
- (35) Lindner, J. H. E.; Kuhn, H. J.; Gollnick, K. Demethylierung von Codein Zu Norcodein Durch Sensibilisierte Photooxygenierung. Tetrahedron Lett. 1972, 13 (17), 1705-1706.
- (36) Gassman, P. G.; Bottorff, K. J. Electron Transfer Induced Desilylation of Trimethylsilyl Enol Ethers. J. Org. Chem. 1988, 53 (5), 1097-1100.
- (37) Crisenza, G. E. M.; Mazzarella, D.; Melchiorre, P. Synthetic Methods Driven by the Photoactivity of Electron Donor-Acceptor Complexes. J. Am. Chem. Soc. 2020, 142 (12), 5461-5476.
- (38) Morris, J. V.; Mahaney, M. A.; Huber, J. R. Fluorescence Quantum Yield Determinations. 9,10-Diphenylanthracene as a Reference Standard in Different Solvents. J. Phys. Chem. 1976, 80 (9), 969-974.
- (39) For Photoexcited State of Enone, See: (a) Turro, N. J.; Ramamurthy, V.; Scaiano, J. C. Modern Molecular Photo- chemistry of Organic Molecules; University Science Books, 2010, 629 - 704. (b) Schuster, D. I.; Lem, G.; Kaprinidis, N. A. New insights into an old mechanism: [2 + 2] photocycloaddition of enones to alkenes. Chem. Rev. 1993, 93, 3-22. (c) Vallavoju, N.; Sreenithya, A.; Ayitou, A. J. L.; Jockusch, S.; Sunoj, R. B.; Sivaguru, J. Photoreactions with a Twist: Atropisomerism-Driven Divergent Reactivity of Enones with UV and Visible Light. Chem. - Eur. J. 2016, 22 (32), 11339-11348.
- (40) For photocatalytic reactivity of thioxanthone, see: (a) Ahuja, S.; Baburaj, S.; Valloli, L. K.; Rakhimov, S. A.; Manal, K.; Kushwaha, A.; Jockusch, S.; Forbes, M. D. E.; Sivaguru, J. Photochemical [2 + 4]-Dimerization Reaction from the Excited State. Angew. Chem., Int. Ed.202463e202316662 (b) Ahuja, S.; Raghunathan, R.; Kumarasamy, E.; Jockusch, S.; Sivaguru, J. Realizing the Photoene Reaction with Alkenes under Visible Light Irradiation and Bypassing the Favored [2 + 2]-Photocycloaddition. J. Am. Chem. Soc. 2018, 140 (41), 13185-13189. (c) Kumarasamy, E.; Raghunathan, R.; Jockusch, S.; Ugrinov, A.; Sivaguru, J. Tailoring Atropisomeric Maleimides for Stereospecific [2 + 2] Photocycloaddition—Photochemical and Photophysical Investigations Leading to Visible-Light Photocatalysis. J. Am. Chem. Soc. 2014, 136 (24), 8729-8737.

- (41) Iyer, A.; Clay, A.; Jockusch, S.; Sivaguru, J. Evaluating Brominated Thioxanthones as Organo-Photocatalysts. *J. Phys. Org. Chem.* **2017**, *30* (9), No. e3738.
- (42) Padwa, A. Intramolecular Cycloaddition of Carbonyl Ylides as a Strategy for Natural Product Synthesis. *Tetrahedron* **2011**, *67* (42), 8057–8072.
- (43) McMills, M. C.; Wright, D. Carbonyl Ylides. In *Synthetic Applications of 1,3-Dipolar Cycloaddition Chemistry Toward Heterocycles and Natural Products*; Chemistry of Heterocyclic Compounds: A Series of Monographs; John Wiley & Sons 2002, 253–314.
- (44) Bos, P. H.; Antalek, M. T.; Porco, J. A., Jr; Stephenson, C. R. J. Tandem Dienone Photorearrangement—Cycloaddition for the Rapid Generation of Molecular Complexity. *J. Am. Chem. Soc.* **2013**, *135* (47), 17978—17982.
- (45) Kanakam, C. C.; Mani, N. S.; Ramanathan, H.; Rao, G. S. R. S. Syntheses Based on Cyclohexadienes. Part 2. Convenient Synthesis of 6-Alkylsalicylates, 6-Alkyl-2,4-Dihydroxybenzoate, and 2,5-Dialkylresorcinols. *J. Chem. Soc. Perkin.* 1 1989, 11, 1907–1913.
- (46) Strieth-Kalthoff, F.; James, M. J.; Teders, M.; Pitzer, L.; Glorius, F. Energy Transfer Catalysis Mediated by Visible Light: Principles, Applications, Directions. *Chem. Soc. Rev.* **2018**, *47* (19), 7190–7202.